

PRF # 57385-ND5

Project Title: Defining Adsorption Energetics of Light Hydrocarbons in Functionalized Metal-Organic Frameworks

P.I. Name, Affiliation: Dr. Michael D. Gross, Wake Forest University

Co-PI, Affiliation: None

### **Progress Report**

Research activities in the second year of this grant focused on two efforts: (1) corroborating experimentally measured adsorption energies of ethane, ethylene, and acetylene on dehydroxylated UiO-66(Zr) metal-organic framework (MOF) having none and  $-\text{NO}_2$  functional groups on the organic linker with simulations and (2) exploring the effect of mixing metals in the MOF-74 structure on the adsorption energies of ethane, ethylene, and acetylene.

In the first year annual report, we experimentally measured a stark difference in the differential energies of acetylene compared to ethane and ethylene at low coverage, in particular for UiO-66- $\text{NO}_2$ . We hypothesized that the observed behavior is due to a strong adsorption site at low coverage that is created by missing organic linker defects, and that we initiated a collaboration with the Thonhauser research group at Wake Forest to computationally predict the effect of missing linker defects on the adsorption of  $\text{C}_2$  hydrocarbons. The first set of simulations were completed on defect-free UiO-66 and UiO-66- $\text{NO}_2$  structures. The predicted adsorption energies from strongest to weakest adsorption energy were ethane > ethylene > acetylene. This was the opposite trend that we observed experimentally. The second set of simulations were completed on UiO-66 and UiO-66- $\text{NO}_2$  with four missing linker defects per zirconium metal cluster. With the missing linker defects, the predicted order of adsorption energies from strongest to weakest were acetylene > ethylene > ethane. Therefore, from a theoretical point of view, we predicted that inducing defects in the UiO-66 structure changes the order of  $\text{C}_2$  hydrocarbon adsorption strength. In the initial experimental work with UiO-66, we did not intentionally induce missing linker defects, nor did we attempt to quantify the number of missing linker defects. During the second year of this grant, we completed additional experimental work to characterize the UiO-66 materials we had already studied and found that the concentration of missing linker defects per metal cluster was one for UiO-66 and two for UiO-66- $\text{NO}_2$ . In an attempt to better understand the adsorption behavior of UiO-66 with a high concentration of missing linker defects, we synthesized new UiO-66 using an acid modulator to purposefully induce missing linker defects. We were able to quantify that our new UiO-66 had three missing linker defects and measured the differential adsorption energies at 293 K and 195 K. We are currently preparing a manuscript with the Thonhauser computational group to report these results. The most important finding is that missing linker defects in the industrially relevant UiO-66 MOF structure have a significant impact on the adsorption behavior of  $\text{C}_2$  hydrocarbons; in particular on the enhanced adsorption strength of acetylene compared to ethane and ethylene, which is important for separating  $\text{C}_2$  hydrocarbons by adsorption.

The exploratory project we conducted in the second year of this grant was the effect of mixing metals on the adsorption behavior of MOF-74. We studied the adsorption of MOF-74 with Ni, Co, Cu, mixed Ni-Cu, mixed Ni-Co, and mixed Co-Cu. The first step in this work was to synthesize the materials. We confirmed the correct MOF-74 structure was synthesized by powder x-ray diffraction. We then used ICP-MS to create a calibration curve of resulting mixed-metal compositions in the MOF-74 structure as a function of precursor concentrations. Finally, we synthesized each mixed-metal MOF-74 material with a targeted composition of 50 atomic % - 50 atomic %. The differential adsorption energy of methane,

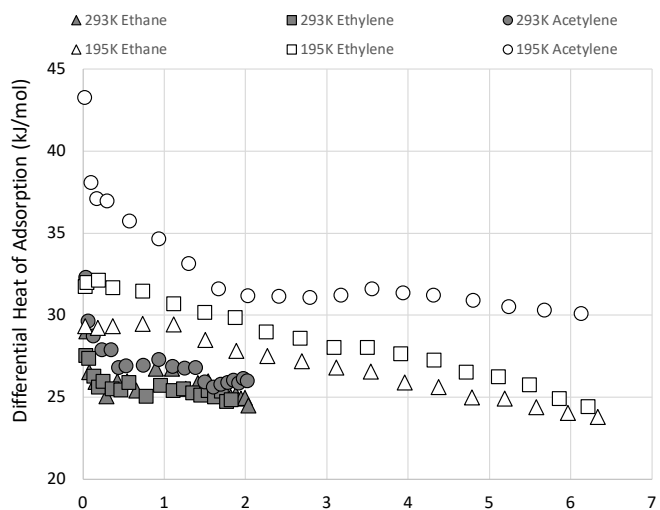


**Figure 1.** Adsorption energies of  $\text{C}_2$  hydrocarbons on UiO-66 with 3 missing linker defects at 293 K and 195 K.

ethane, ethylene, acetylene, and carbon dioxide on each MOF-74 was measured as a function of coverage. Carbon dioxide was measured as a reference point because the heat of adsorption of carbon dioxide on Co-MOF-74 and Ni-MOF-74 are widely accepted in the literature. For the hydrocarbons, either there is little experimental data or none for these MOF-74 materials. A summary of our results is shown in Table 1.

We hypothesized that the mixed-metal MOF-74 would have an adsorption energy in between the single-metal adsorption energies. This hypothesis was proven incorrect. In general, the mixed-metal adsorption energies closely matched the single-metal Cu-MOF-74 adsorption energies. Our experimental measurements matched the well accepted literature values for carbon dioxide adsorption on Co-MOF-74 and Ni-MOF-74; however, our experimental results for hydrocarbon adsorption were drastically different in some cases. For example, the adsorption energy of acetylene on Ni-MOF-74 was measured to be 51 kJ/mol and the theoretically predicted adsorption energy was 37 kJ/mol, a 38% discrepancy in the strength of adsorption. We also observed a large difference in adsorption energy of 16.5 kJ/mol between ethane and ethylene for Ni-MOF-74 compared to a theoretically predicted difference of 5 kJ/mol. A similar discrepancy in adsorption energy difference was found for Co-MOF-74. This larger difference in adsorption energy between ethane and ethylene could be important for their separation by adsorption. We have asked the Thonhauser computational research group to help us understand the nature of the discrepancy between theoretical adsorption energy and experimental.

The last item to report is that our collaborations with the Thonhauser group recently initiated a new project. We have asked for a one year extension on this grant and during that time we will study the adsorption behavior of C<sub>2</sub> hydrocarbons on UTSA-300 by calorimetry. This material has been shown to adsorb acetylene and completely block ethylene and has a gate-opening effect. The adsorption behavior during gate-opening cannot be studied by traditional isosteric heat calculations from isotherms. Therefore, we will directly measure heats of adsorption as a function of coverage in this region with calorimetry.

### **Impact on Career and Students**

This New Directions grant has already made a significant impact on my career. The adsorption calorimetry work was indeed a brand new direction of scholarly work for me. With the support of this grant, I was able to establish a home-built experimental technique that is only available to a handful of research groups in the country. In the second year, we have observed intriguing results for the adsorption of C<sub>2</sub> hydrocarbons on two different MOF structures. We have also strengthened our collaboration with a highly respected computational group in the MOF adsorption field. The collaborative approach of closing the feedback loop between computational modeling, synthesis, and experimental characterization has a high likelihood for success for future research. The grant has supported a graduate student on a full time basis. The graduate student presented this research at SERMACS in spring 2019 and successfully defended their thesis in May of 2019. A journal manuscript on the research is currently underway and a second manuscript is expected to be submitted during the one year extension of this grant. In addition to the graduate student support, one undergraduate student gained research experience over the summer. The undergraduate student worked alongside the PI learning about the theory and instrumentation as well as conducting all facets of the experimental work, including synthesis, activation, and characterization.

**Table 1.** A comparison of experimental and theoretical adsorption energies on single-metal and mixed-metal MOF-74.

		Methane	Ethane	Ethylene	Acetylene	CO <sub>2</sub>
Co	Theoretical	18	35	38	36	34
	Experimental	16.5	30	43.5	42.5	33
Ni	Theoretical	19	36	41	37	37
	Experimental	17	29	45.5	51	37
Cu	Theoretical	14	27	22	20	27
	Experimental	10.5	21	24	25.5	17.3
Co-Ni	Theoretical	18-19	35-36	38-41	36-37	34-37
	Experimental	15	29	46	42	36
Ni-Cu	Theoretical	14-19	27-36	22-41	20-37	27-37
	Experimental	9.6	21.5	25.5	28.6	21
Co-Cu	Theoretical	14-18	27-35	22-38	20-36	27-34
	Experimental	8.5	19	25.5	29.3	23